Dynamics of Ethylene Glycol in Antifreeze Mixtures

HFBS Team: Madhu Tyagi, Timothy Prisk and Richard Azuah

Abstract

In this experiment, we will use incoherent quasi-elastic neutron scattering to examine the dynamics of antifreeze mixtures. We will use heavy water to mask the signal from water and study self-diffusion and molecular orientation of ethylene glycol in these mixtures. The goal of this hands-on experiment is to learn how to selectively explore component dynamics in a liquid mixture as well as an understanding and appreciation of neutron backscattering spectroscopy. In addition, we will learn how to collect, analyze, and interpret this type of data.

1 Introduction

Quasi-elastic neutron scattering techniques provide experimentalists with direct probes of the atomic-scale dynamics of materials[1]. These methods are especially sensitive to the motion of hydrogen atoms, as the incoherent scattering cross section of hydrogen is very large compared to other nuclei. The corresponding cross section for deuterium atoms is relatively low, making *selective deuteration* a useful technique when studying multi-component systems or systems with inequivalent hydrogen atoms. For example, when studying binary liquid mixtures, selective deuteration enables one to examine the dynamics of each component of the mixture separately. In this summer school experiment, we will use neutron backscattering and selective deuteration to study the molecular motions of ethylene glycol in antifreeze solutions.

Ethylene glycol ($HOCH_2CH_2OH$) is a low-molecular weight organic liquid that is widely used as as a deicing fluid and automobile antifreeze. These applications of ethylene glycol are based upon the fact that its freezing point is depressed when mixed with water. Figure 1 plots the freezing point of the mixtures against the number of water molecules per ethylene glycol molecule. The minimum freezing point occurs near a ratio of 2.5:1 (two and a half water molecules to one glycol molecule).

In addition to their technological relevance, mixtures of ethylene glycol and water have intrinsic interest as examples of two-component hydrogen bonding liquids. Ethylene glycol possesses two hydroxyl groups and two oxygen atoms which can serve as donors and acceptors of hydrogen bonds, respectively. Matsugami *et al* have carried out small-angle neutron scattering and pair-distribution function studies of the structure of ethylene glycol and water mixtures[3]. Their SANS data indicates that ethylene glycol and water mix homogeneously; they do not form clusters in solution. From their pair-distribution function measurements, they conclude that the ethylene glycol molecules adopt a gauche conformation. A plausible model of the hydrogen bond chain in liquid ethylene glycol is shown in Figure 2. The network is not merely a one-dimensional chain, but a three-dimensional branched structure. A general discussion of the physics and chemistry of hydrogen bonding may be found in the book by Maréchal[4].

Since the phase behavior and microscopic structure of water-glycol mixtures have been characterized, we will proceed in this neutron scattering experiment to examine the dynamics underlying these mixtures. We will use heavy water (D_2O) instead of light water (H_2O), thereby "masking" the scattering from the water.

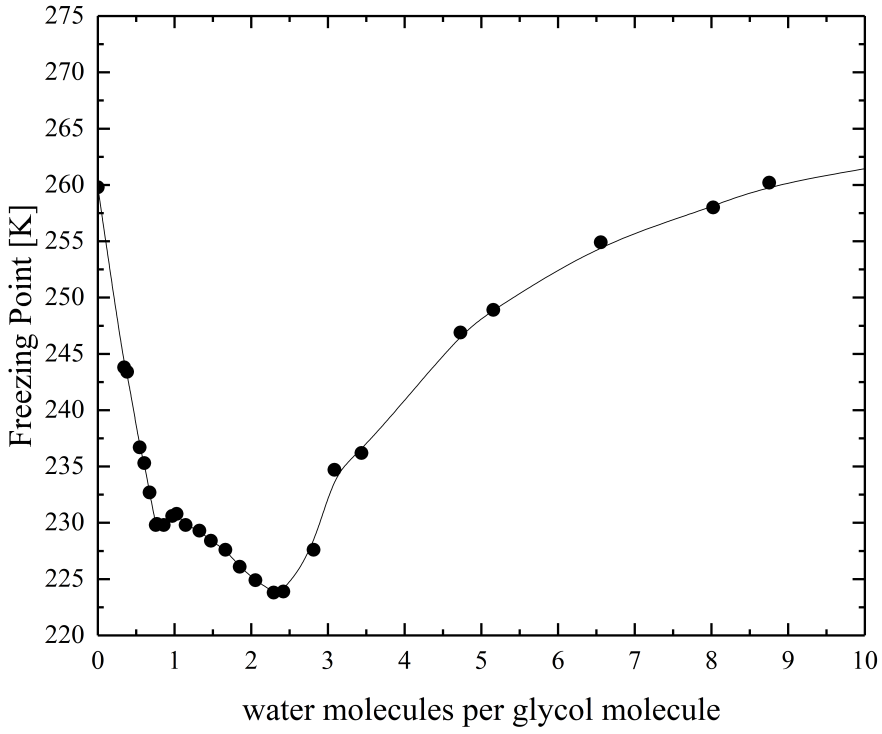

Figure 1: The freezing point of water and ethylene glycol mixtures plotted against the ratio of water molecules to glycol molecules. The solid lines are spline fits to the freezing points reported in Ref [2].

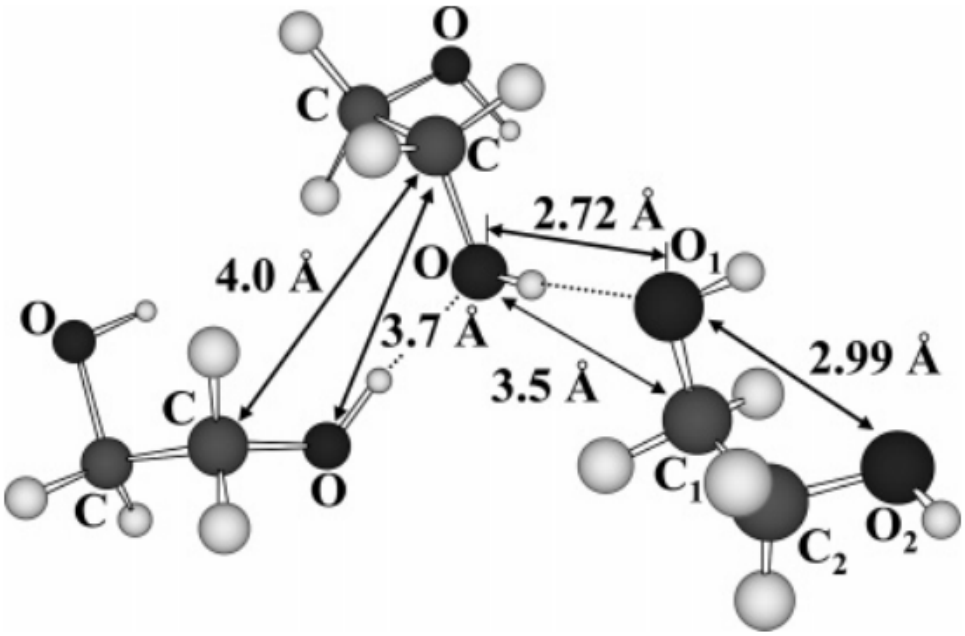

Figure 2: Hydrogen bond chain within liquid ethylene glycol[3].

2 Why Use Neutron Backscattering?

When planning a neutron scattering experiment, one should consider whether a given spectrometer is appropriate for carrying out the study. The High Flux Backscattering Spectrometer (HFBS) is well-suited to the study of viscous liquids because of the length and time scales probed by the instrument. The momentum $\hbar Q$ and energy $\hbar\omega$ transfer are inversely proportional to the length and time scales under observation, respectively. HFBS spans a dynamic range of $0.25\ \text{Å}^{-1} \leq Q \leq 1.75\ \text{Å}^{-1}$ and $-36\ \mu\,\text{eV} \leq E \leq +36\ \mu\,\text{eV}$. This corresponds to length scales between 25 Å and 3.6 Å and time scales between 2 ns and 0.1 ns. As we will see, this means that HFBS can be used to study liquids with self-diffusion constants on the order of $10^{-3}\ \text{Å}^2/\text{ps}$. For slower motions, it may be advisable to pursue neutron spin echo; for faster motions, consider the Disk Chopper Spectrometer.

3 What will we do in this experiment?

Ethylene glycol ($HOCH_2CH_2OH$) is a small-molecule organic liquid which is available commercially. We have prepared mixtures of heavy water (D_2O) and ethylene glycol with the following ratios of heavy water molecules to ethylene glycol molecules: 0:1; 1:1; 2:1. Each of these mixtures was loaded into an aluminum sample can with a 0.1 mm annulus. The sample can was sealed with indium under an ambient atmosphere.

The sample geometry was chosen to minimize the amount of *multiple scattering*. In an ideal neutron scattering measurement, we would like for the neutron to scatter once within the sample before reaching the detector. In practice, neutrons can undergo several scattering events within the sample and/or be absorbed by the sample. The number of events increases with the thickness of the sample illuminated by the beam. One often used rule-of-thumb is to select the sample geometry so that 90% of the incident neutrons are transmitted in the forward direction. This is often a good compromise between signal and the effects of multiple scattering. Such as a sample is informally referred to as a *10% scatterer*.

The DAVE software package has a planning tool for estimating the macroscopic scattering cross section Σ of a sample of known chemical composition. It also has a tool for estimating the amount of multiple scattering and the size of self-shielding corrections. For ethylene glycol ($C_2H_6O_2$) at a density of 1.13 g/cc, the macroscopic scattering cross sections are: $\Sigma_{\text{inc}} = 5.28\ \text{cm}^{-1}$, $\Sigma_{\text{coh}} = 0.33\ \text{cm}^{-1}$; and $\Sigma_{\text{abs}} = 0.02\ \text{cm}^{-1}$. The incoherent scattering from hydrogen makes largest contribution to the total macroscopic cross section Σ_{tot}, and so our measurements are primarily sensitive to the self-correlation function of the hydrogen atoms.

Using the planning tools in DAVE, estimate the macroscopic scattering cross section, strength of single and double scattering, and the self-shielding factor.

The sample will be placed in a top-loading closed-cycle refrigerator capable of reaching a base temper-ature of 4 K. We will use a low-T stick to cover the temperature range between 4 K and 300 K. This will be demonstrated via a virtual experiment.

On HFBS, how many times does the beam go through the sample before reaching the detectors?

The answer to this question can have important consequences for your experiment. If the beam pases through the sample twice (for instance) and the sample has an appreciable neutron absorption cross section, then the intensity at the detectors will be lower than if the beam had only passed once through the sample. Additionally, a beam which passes twice through a strongly scattering sample can produce an energy-dependent background. For more details on these points, see the appendices.

4 Modes of Spectrometer and Data Reduction Details

We can use HFBS in two different modes to extract the dynamical features of the sample under investigation. A detailed description of the spectrometer is given in Ref [5].

4.1 Fixed Window Scans

For reactor based neutron backscattering spectrometers, “Fixed window scans” or “elastic scans” are very powerful for getting a fast overview of the dynamics of a system and are often the starting point for quasi-elastic measurements. In this mode, we choose to count the neutrons with fixed initial and final wave vectors which results in analyzing neutrons scattered within a fixed energy window. To do so, we stop the moving monochromator (see below) and then change the external parameters like temperature and pressure and record the intensity. We can even assign a time scale to fixed window scans based on the instrumental resolution. In our case, assuming a FWHM of about 0.8 μeV, the slower limit would correspond to 2 ns. Dynamic processes on a time scale slower than the instrumental resolution are not resolved and thus are counted within the ”elastic window”. Faster motions of scattering particles can be resolved and will induce an energy loss or gain of the scattered neutrons, which then are no longer reflected by the analyzers to the detectors. One observes a decrease of the elastic window intensity as function of increasing temperature. Therefore, elastic or fixed window scans give a quick overview of the onset of motions faster than the time scale corresponding to the energy resolution and therefore, can be used to choose suitable temperatures for dynamic measurements.

4.2 Quasi-elastic Neutron Scattering

The HFBS spectrometer is configured in an inverse scattering geometry. This means that the energies of the neutrons incident on the sample are varied while the final energy of the neutrons reaching the detectors is fixed.

A summary of the basic principle of operation of HFBS is outlined below (for more details on the instrument including a schematic see Appendix B and Ref[5]).

1. The "white" beam of neutrons produced by the reactor is velocity selected to yield neutrons that have energies around the desired energy of 2.08 meV. These neutrons are further focused in energy by a rotating phase space transform chopper and scattered towards the Doppler monochromator. The energy focused neutrons are backscattered from the Doppler monochromator thus selecting incident neutron energies, E_i, dependent upon the speed of the monochromator when reflected. While the Doppler is at rest, only neutrons with energies of 2.08 meV are backscattered from the monochromator. This is due to the lattice spacing of the Si hexagons that tile the surface of the monochromator.

2. The reflected neutrons from monochromator interact with the sample and are scattered from the sample with a distribution of energies.

3. Only neutrons with a particular scattered energy, E_f, reflect from the analyzer array into the detectors. Identical Si hexagons comprise the analyzer system, thus the backscattered neutrons all have energies of 2.08 meV. The energy transfer imparted on the sample is defined as $E = E_i - E_f$.

4. Neutrons scattered from the sample in a particular direction backscatter from particular analyzers and are counted one of the 16 detectors. This direction corresponds to the scattering angle, 2θ.

What is the energy range of the neutrons incident on the sample, $E_i \pm \delta E_i$?

Given the scattering angle 2θ and energy transfer E, we may calculate the magnitude of the momentum transfered to the sample Q. Kinematical arguments lead to the following relationship between 2θ, E, E_i, and Q:

$$\frac{\hbar^2 Q^2}{2m} = 2E_i - E - 2\sqrt{E_i(E_i - E)}\cos(2\theta), \tag{1}$$

where m is the mass of the neutron.

The data acquisition system records the number of detector counts as a function of initial neutron velocity, v_i, where v_i is related to the instantaneous monochromator velocity, v_m, and the Bragg velocity of the neutrons with velocity 630 m/s, v_B, via $v_i = v_B + v_m$. The energy transfer to the sample, due to a Doppler shift of the neutron energies, is given by

$$E = 2E_B\left(\frac{v_m}{v_B}\right) + E_B\left(\frac{v_m}{v_B}\right)^2 \tag{2}$$

where E_B is the Bragg energy of neutrons with wavelength 6.27 Å, is written to the raw data file. This calculation is done using an encoded Doppler drive that provides information as to the acceleration as a function of position. The energy change is derived from this acceleration. Note that the motion of the monochromator is time-dependent, allowing the variation of E_i necessary to an inverse geometry spectrometer.

HFBS exploits the Doppler effect to vary the incident neutron energies. Can you think of an alternative technique? How would one design a backscattering spectrometer if the monochromator were set up to be stationary?

The raw data is recorded as $N(2\theta_j, E_k) = N_{j,k}$, the number of neutrons detected in detector j (at scattering angle corresponding to $2\theta_j$) with an energy transfer to sample of E_k. The quantity which reflects the dynamics of the scattering system most directly is $S(Q, E)$, the dynamic structure factor. What we measure, $N_{j,k}$, is closely related to the double differential scattering cross section $d^2\sigma/d\Omega dE$. This can

be written in terms of various instrument-dependent parameters and the number of counts received in the detectors.

$$\left[\frac{d^2\sigma}{d\Omega dE}\right]_{j,k} = N_{j,k}\frac{A\eta(FC)}{N(FC)}\frac{\gamma_j}{\eta(E_f)}\frac{1}{\rho_N V}\frac{1}{\Delta\Omega_j}\frac{1}{\Delta E}. \tag{3}$$

Here,

- $\frac{A\eta(FC)}{N(FC)}$ is the *monitor normalization* of the incident beam area A times the beam monitor efficiency $\eta(FC)$ divided by the numebr of counts recieved by the beam monitor. 'FC' indicates the type of detector, a fission chamber.
- $\frac{\gamma_j}{\eta(E_f)}$ is the *vanadium normalization* of the detector intensity with the intensity scaling factor γ_j divided by the efficiency of the detector.
- ρ_N is the number density of scatterers in the sample.
- V is the volume of sample illuminated by the beam.
- $\Delta\Omega_j$ is the solid angle subtended by detector or analyzer angular coverage.

We obtain the dynamic structure factor $S(Q,E)$ using the first Born approximation (i.e. a single scattering event dominates the response of the sample).

$$S(Q,E) = \frac{4\pi}{\sigma}\frac{k_i}{k_f}\frac{d^2\sigma}{d\Omega dE}. \tag{4}$$

Here σ is the scattering cross section of the sample and $k_i(k_f)$ is the incident (final) neutron wavevector.

An important relationship exists between neutron downscattering ($E > 0$) and neutron upscattering ($E < 0$) known as the *principle of detailed balance*. Suppose that the sample is in thermal equilibrium at temperature T. Then, $S(Q,E)$ obeys the following condition:

$$S(Q,-E) = e^{-E/k_BT}S(Q,E) \tag{5}$$

In general, the dynamic structure factor $S(Q,E)$ is asymmetric with respect to energy transfer E. The probability that a neutron will upscatter with energy transfer E is smaller than the probability that a neutron will downscatter with energy transfer E by a thermal factor e^{-E/k_BT}.

How will the principle of detailed balance affect our observations in this experiment? Assess the importance of the detailed balance effect in the energy window of HFBS for temperatures above 200 K. ***Hint****: 1 meV = 11.6 K.*

5 Analysis and Interpretation of the Scattering Data

5.1 Fixed Window Scans

We will begin our analysis of the experimental data with the fixed window scans.

You may notice abrupt, step-like changes in the $I_{el}(Q,T)$ of your samples. Are these physically real or are they merely artifacts? What is happening in the samples at these steps?

The fixed window scan data may be used to estimate the mobility of hydrogen atoms in our samples on the time-scale scale probed by HFBS. We suppose that the elastic intensity $I_{el}(Q,T)$ decays from its value at zero temperature $I_e(Q,0)$ according to Debye-Waller factor:

$$I_{el}(Q,T) = I_{el}(Q,0)\exp\left(-\frac{Q^2\langle u\rangle^2}{3}\right) \tag{6}$$

Here $\langle u^2\rangle$ is the effective mean-squared displacement of the hydrogen atoms. This quantity may be estimated by plotting:

$$-3\ln\left(\frac{I_{el}(Q,T)}{I_{el}(Q,0)}\right) \text{ vs. } Q^2 \tag{7}$$

The effective mean-squared displacement $\langle u^2\rangle$ is given by the slope of the line formed by the data.

How do you expect $\langle u^2\rangle$ to vary with temperature when the dynamics are too slow to be resolved? And how about when the dynamics of the system are within the experimental time window?

5.2 van Hove correlation functions

Recall that, in a neutron spectroscopy experiment, one measures the double-differential scattering cross section:

$$\frac{d^2\sigma}{d\Omega dE_f} = \frac{1}{4\pi}\frac{k_f}{k_i}\underbrace{\left(\sigma_{coh}S_{coh}(\mathbf{Q},E) + \sigma_{inc}S_{inc}(\mathbf{Q},E)\right)}_{S(\mathbf{Q},E)} \tag{8}$$

The dynamic structure factor $S(\mathbf{Q},E)$, or scattering law, is the sum of the *coherent* dynamic structure factor $S_{coh}(\mathbf{Q},E)$ and the *incoherent* dynamic structure factor $S_{inc}(\mathbf{Q},E)$, each weighted according to their respective cross sections. $S_{coh}(\mathbf{Q},E)$ is the Fourier transform of the time-dependent *pair*-correlation function $G_P(\mathbf{r},t)$. In a classical liquid, this function has the following physical meaning. Given an atom at the origin $(0,0)$, $G_P(\mathbf{r},t)$ is the relative probability of finding *another* atom at $(\mathbf{r},t)$. Meanwhile, $S_{inc}(\mathbf{Q},E)$ is the Fourier transform of the time-dependent *self*-correlation function, $G_S(\mathbf{r},t)$. Given an atom at the origin $(0,0)$, the self-correlation function is the relative probability of *that same atom* being located at position $\mathbf{r}$ at time t.

In our experiment, two simplifications can be made to Equation 8. First, bulk liquids are homogenous and isotropic. Accordingly, we do not need to consider the vector quantities $\mathbf{Q}$ and $\mathbf{r}$. Instead, we can work with the scalar quantities Q and r. Second, we have already seen that the incoherent scattering cross section Σ_{inc} of our sample is much larger than the coherent scattering cross section Σ_{coh}. We may neglect the contribution of coherent scattering to $d^2\sigma/d\Omega dE_f$. Therefore, we are determining the incoherent dynamic structure factor $S_{inc}(Q,E)$ in this experiment, which will hereafter simply be referred to as $S(Q,E)$.

In order to interpret the scattering data, one introduces a model for the time-dependent self-correlation function $G_S(r,t)$. There are several approaches to developing such a model. For example, one might perform realistic simulations of the system using classical molecular dynamics. In that case, $G_S(r,t)$ may be calculated from the simulated trajectories of the hydrogen atoms. Another approach, which is the one we will adopt here, is to write down an analytic expression which describes the motion. In this phenomenological approach, our expression will contain several adjustable parameters, such as the self-diffusion constant D_T. The values of these adjustable parameters are estimated by means of a least-squares fit to the experimental data. In fact, we will ultimately consider two phenomenological models.

Suppose that we are studying the diffusion of an atom in a classical monoatomic liquid. This means that we are examining length scales which are longer than the elementary diffusion steps and time scales which

are longer than the jump time. In case, the atoms obey *Fick's Law*:

$$\frac{\partial \rho(\mathbf{r},t)}{\partial t} = D_T \nabla^2 \rho(\mathbf{r},t). \tag{9}$$

Here ρ is a number density of particles and D_T is the (translational) *diffusion constant*. If we take $\rho(\mathbf{r},0)$ to be $\delta(\mathbf{r})$, then we may identify interpret ρ as a probability density – that is, as $G_S(r,t)$. (You may recognize this as the problem of finding the Green's function for the diffusion equation.) In that case, the solution of Equation 9 is:

$$G_S(r,t) = \frac{1}{(4D_T t)^{3/2}} \exp\left(\frac{-r^2}{4D_T t}\right) \tag{10}$$

Therefore, if the particles obey the diffusion equation and start at a common location, then they will spread out in space in a Gaussian distribution. The width of that distribution is proportional to $D_T t$.

If we first take the Fourier transform with respect to position, then we obtain the intermediate dynamic structure factor:

$$\widetilde{S}(Q,t) = \exp\left(-t/\tau(Q)\right) = \exp\left(-D_T Q^2 t\right) \tag{11}$$

Taking the Fourier transform with respect to time leads us to:

$$S_T(Q,E) = \frac{1}{\pi} \frac{\Gamma_T/2}{(\Gamma_T/2)^2 + E^2} \tag{12}$$

This lineshape is known as a *Lorentzian*. Γ is the full-width at half-maximum (FWHM) of the Lorentzian. For translational diffusion, $\Gamma_T(Q) = 2\hbar Q^2 D_T$.

5.3 Model A: Decoupled Translational and Rotational Diffusion

In an organic molecular liquid, the incoherent dynamic structure factor depends upon a combination of the translational and rotational motion of the hydrogen atoms. If these motions are uncorrelated, then the dynamic structure factor may be expressed as a convolution of two functions, one describing the translational motion of the molecule and another describing the rotational function of the molecule: $S(Q,E) = S_T(Q,E) \otimes S_R(Q,E)$. We have already seen that, for long-range translational diffusion, $S_T(Q,E)$ may be expressed as a Lorentzian function with a FWHM of $\Gamma_T(Q) = 2\hbar Q^2 D_T$. What can we expect from $S_R(Q,E)$?

A number of different models for $S_R(Q,E)$ have been developed in the literature, each appropriate to a particular type of molecular reorientation: isotropic rotational diffusion, jump diffusion along N sites on a circle, reorientations of molecules about different axes in space, and others. A discussion of these models may be found in the book by Bée[6]. We will not examine any of these models in detail, but will instead infer the general characteristics of $S_R(Q,E)$ from the qualitative character of $G_S(r,t)$.

Consider the motion of a hydrogen atom which is part of a rotating molecule. As the molecule rotates, the hydrogen atom moves along a spherical surface in space. Initially, $G_S(r,0) = \delta(r)$. After a short time $G_S(r,t)$ decays from its initial value as the hydrogen atom randomly wanders away from its starting position. At long times, $G_S(r,t)$ approaches a constant value. Because the hydrogen atom is restricted to moving along the surface of a sphere, there are correlations between $t = 0$ and $t = \infty$. This is unlike translational diffusion, where $G_S(r,t)$ goes to zero at infinite time. Thus, we may write down a model for the intermediate dynamic structure factor:

$$\widetilde{S}_R(Q,t) = EISF(Q) + (1 - EISF(Q)) \exp\left(-t/\tau\right) \tag{13}$$

Here we have assumed an exponential relaxation with a characteristic time τ. It is inversely proportional to the rotational diffusion constant $D_r = 1/\tau$. The Elastic Incoherent Structure Factor (EISF) is determined by the geometry of the motion. While we will not attempt to analyse the EISF in this summer school experiment, obtaining the EISF often allows experimenters to classify the type of molecular rotation being observed.

Again, assuming that translational and rotational motion are decoupled, the dynamic structure factor of our system is given by:

$$\widetilde{S}(Q,t) = \widetilde{S}_T(Q,t)\widetilde{S}_R(Q,t) \quad (14)$$

$$S(Q,E) = S_T(Q,E) \otimes S_R(Q,E) \quad (15)$$

Derive an explicit expression for $S(Q,E)$. How does the result differ from Equation 12?

Obtain empirical estimates of the translational D_T and rotational D_R diffusion constants as a function of composition and temperature. ***Hint****: $\Gamma_T(Q) = 2\hbar DQ^2$ and $\Gamma_R(Q) = 2\hbar D_r$.*

In many cases, the diffusion constant obeys an Arrhenius law:

$$D = D_0 e^{-E_A/k_B T} \quad (16)$$

where E_A is the activation energy.

Do the diffusion constants obey an Arrhenius law? If so, how does the activation energy E_A vary amongst the samples? ***Hint****: Plot $\log D$ versus $1/T$.*

5.4 Model B: Stretched Exponential Relaxation

The analysis of the previous section turned on several assumptions: (1) the translational and rotational motions of the molecules are completely uncorrelated; (2) each type of motion undergoes exponential relaxation $\exp(-t/\tau)$ with a *single* relaxation time τ for each value of Q. However, there are many systems for which one or both of these assumptions may not be valid. Therefore, we we will consider an alternative model for $S(Q,E)$.

It has been found empirically that the intermediate dynamic structure factor $\widetilde{S}(Q,t)$ of many systems (e.g. glass formers, polymers, biological macro-molecules) may be described by the *Kohlrausch-Williams-Watts* (KWW) function or stretched exponential:

$$\widetilde{S}(Q,t) = \exp\left(-(t/\tau)^\beta\right) \quad (17)$$

In general, β may assume any value between zero and one. Unfortunately, there is no known closed analytic expression for $S(Q,E)$, except for $\beta = 1/2$ or $\beta = 1$.

Two different reasons for the stretched exponential form have been proposed in the literature[7]. First there is the homogeneous scenario: all of the particles in the system relax identically to one another, but the relaxation is not purely exponential. For example, if the particles undergo fractal diffusion, then $\langle r(t)\rangle = 6Dt^\beta$ and $1/\tau(Q) = (DQ^2)^{1/\beta}$. On the other hand, there is the heterogeneous scenario: there is a distribution of relaxation times within the system. In this case, we express $\widetilde{S}(Q,t)$ as a superposition of different exponential relaxations, weighted by an appropriate distribution g of relaxation times:

$$\exp\left(-(t/\tau)^\beta\right) = \int_{-\infty}^{+\infty} g(\ln\tau') e^{-t/\tau'} d\left(\ln\tau'\right) \quad (18)$$

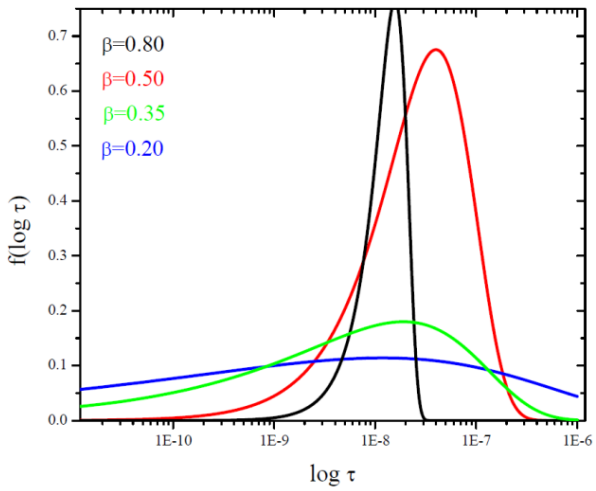

Figure 3: Distributions of relaxation times in the heterogeneous scenario.

Figure 3 plots the distribution function $g(\ln \tau)$ for different values of the stretching parameter β. In the limiting case where $\beta \rightarrow 0$, the distribution approaches a δ-function. As β increases, the width of the distribution increases.

We will analyze our scattering data according to Equation 17. Because there is no known closed analytic expression for $S(Q, E)$, it is necessary to carry out the Fourier transform numerically. One option to perform a Fast Fourier Transform upon the experimental data itself and obtain the intermediate dynamic structure factor. However, there are many sources of systematic errors associated with the Fourier transform of noisy data. A better option in this case is to transform the stretched exponential model of $\widetilde{S}(Q, t)$ to $S(Q, E)$. There is a fitting function in DAVE, namely ft_KWW, which does precisely this.

Obtain empirical estimates for the stretching exponent β and relaxation times τ as a function of temperature and composition. Compare these relaxation times to the values you obtain from Model A.

Fit the relaxation times to a power law: $\tau(Q) = \tau_0 Q^{-\gamma}$. What do you obtain for γ?

A Effects of the Sample Geometry on Self Shielding and Multiple Scattering

One must consider a number of issues when determining appropriate sample geometry. A naïve philosophy in designing sample geometry is to make the sample as big as possible in order to obtain as many scattering events in the shortest possible time. Unfortunately, optimization of the experiment is not as simple as this. Sample design involves careful consideration of the composition of the sample in terms of its scattering and absorption cross sections.

In order to understand the extent to which you have to correct for multiple scattering/self-shielding, it is important to know how strong a scatterer/absorber your sample is. The transmission in the forward direction ($2\theta = 0$) is often calculated and expressed in terms of a percentage of the incident beam that is scattered/absorbed. Suppose that the sample has a microscopic bound scattering cross section $\sigma_{tot} = \sigma_{inc} + \sigma_{coh}$ and microscopic absorption cross section σ_{abs}. Then, the macroscopic scattering Σ_S and absorption Σ_A cross sections (in units of cm^{-1}) are given by:

$$\Sigma_S = \sigma_{tot}\rho \tag{19}$$

$$\Sigma_A = \sigma_{abs}\rho, \tag{20}$$

where ρ is the molar density of the atoms. For a flat plate sample of thickness t at an angle ϕ to the incident beam, the probability S of scattering is:

$$S = \frac{\Sigma_S}{\Sigma_T}\left(1 - e^{-\Sigma t \sec\phi}\right) \tag{21}$$

For a thin annular cell,

$$S = \frac{\Sigma_S}{\Sigma_T}\left(1 - e^{-\pi\Sigma_T t}\right) \tag{22}$$

We illustrate the self-shielding corrections for a vanadium sample in the flat plate and annular geometries, where $\sigma_{tot} = 5.10$ barns and $\sigma_{abs} = 5.08$ barn for 1.8 Å neutrons. The intensity in the detectors is very sensitive to the thickness t of the sample as well as its geometry. If we assume for these two geometries the same amount of scattering (5%, 10%, and 20% scatterers) and assume that the samples are completely illuminated by the incident beam, then we obtain the results shown in Figure 4. The corrected intensity is obtained using $I_{corr}(2\theta, E) = I_{obs}(2\theta, E)/A_{ssc}$, where $I_{obs}(2\theta, E)$ is the observed intensity. It is quite clear that there is a much stronger angle dependence for the correction factor of the slab geometry whereas the corrections are much less for the annular cell. Furthermore, an evaluation of the correction factor is impossible near the orientation angle, 130° in the present example, for the slab geometry. Therefore, it is advantageous to use an annular geometry for backscattering.

Corrections for multiple scattering are not trivial and, for many systems in which the scattering function is not known *a priori*, may not be possible at all. Figure 5 illustrates the effects that multiple scattering can have on a system, in this case viscous glycerol. This sample was measured on the IN10 backscattering spectrometer at the ILL where structural relaxation (viscous flow) is on the time scale of tenths of nanoseconds. There is clear broadening of the lineshape with increasing Q due to the dynamics of the system. However, at $Q = 0.19$ Å^{-1}, structural relaxation cannot be resolved because it is too slow at this small Q. The apparent broadening in the wings is entirely due to multiple scattering.

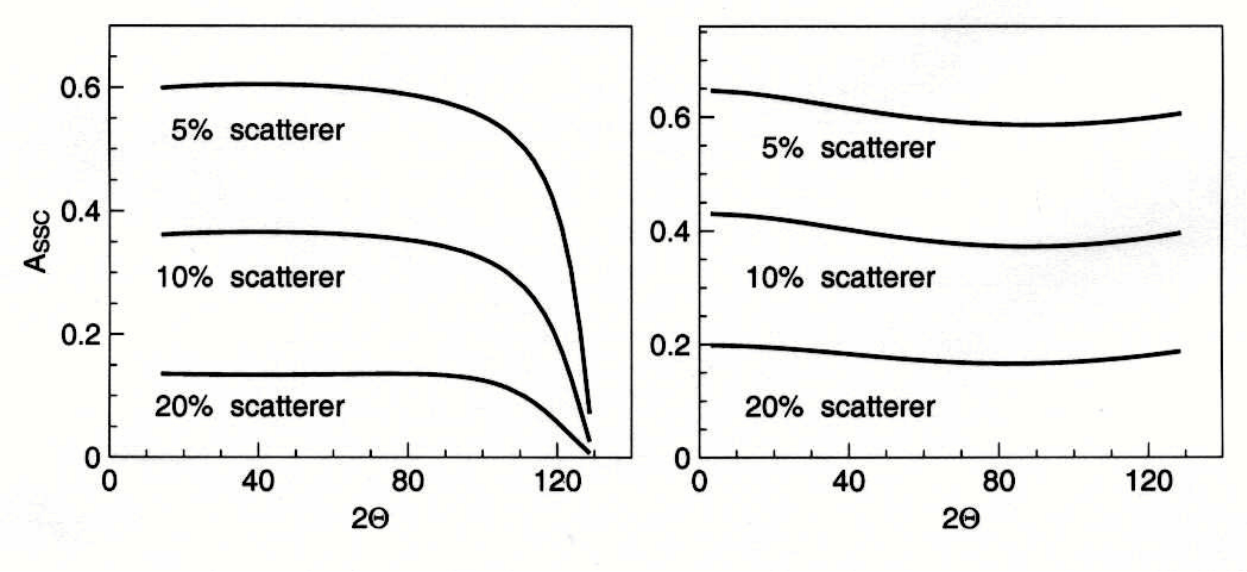

Figure 4: The self-shielding factor as a function of scattering angle 2θ are compared: flat plate oriented at 130° to the incident beam (left) and a thin annulus.

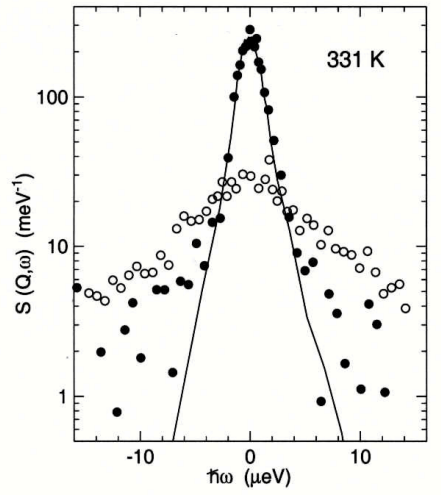

Figure 5: Scattering intensity of viscous glycerol taken on the IN10 backscattering instrument illustrating the effects of multiple scattering on $S(Q, E)$[8] . Solid line represents the instrumental resolution, open symbol are data taken at $Q = 1.4$ Å^{-1} and the closed symbols are data taken at $Q = 0.19$ Å^{-1}.

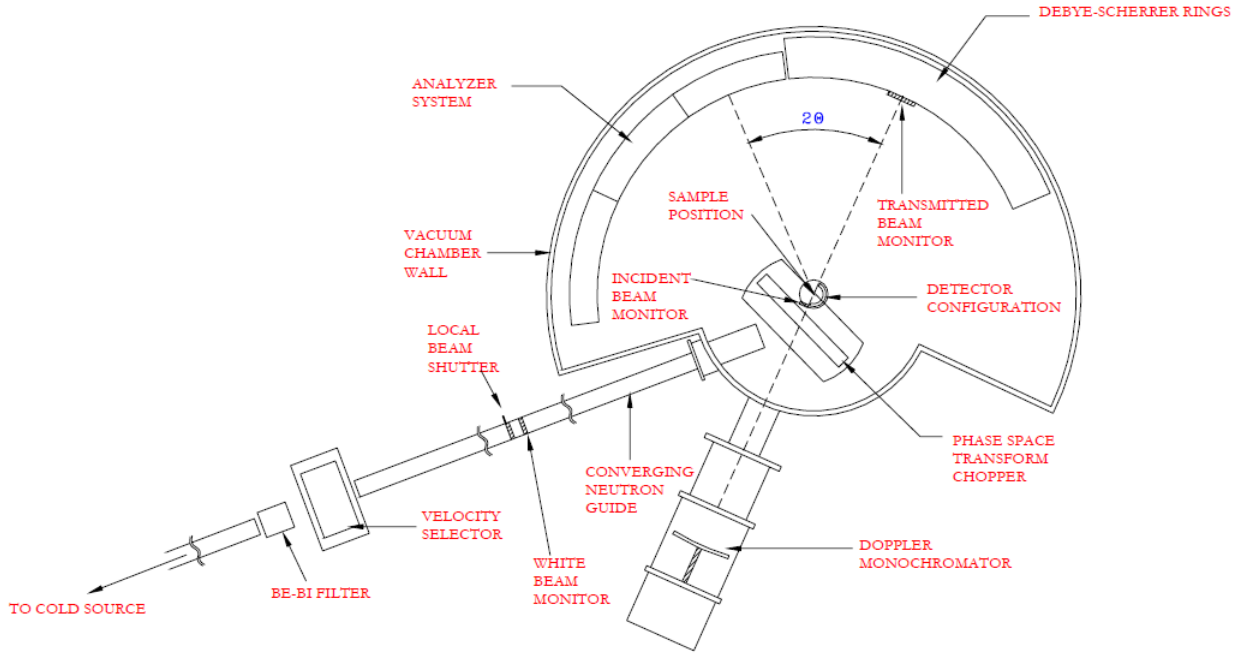

Figure 6: Schematic of the High Flux Backscattering Spectrometer[5].

B Characteristics of the High Flux Backscattering Spectrometer

- Website: http://www.ncnr.nist.gov/instrument/hfbs
- Si (111) analyzers cover 20% of 4π steradians.
- $\lambda = 6.27$ Å
- $E_f = 2.08$ meV
- $v_n = 630$ m/s
- 16 ^{3}He detectors covering $14^\circ \leq 2\theta \leq 121^\circ$
- Dynamic range: 0.25 Å$^{-1} \leq Q \leq 1.75$ Å^{-1}; $-36\ \mu$ eV $\leq E \leq +36\ \mu$ eV.
- Instrumental resolution: $\delta Q = 0.1$ Å$^{-1} - 0.2$ Å^{-1}; $\delta E \leq 1\ \mu$ eV
- Flux at sample: $\Phi \approx 1.4 \times 10^5$n/cm^2/s
- Beam Size at Sample: 2.8 cm by 2.8 cm.
- Signal-to-noise: 400:1 for vanadium foil (10% scatterer).
- Standard sample environments: Closed cycle refrigerator (5 K to 325 K); Closed cycle refrigerator (50 K to 600 K); Orange cryostat (1.5 K to 300 K).

C Instrumental Resolution

In an experiment with an ideal instrument, we could measure the sample's scattering response directly. However, real neutron spectrometers (or any measurement apparatus) have finite resolution which distorts the measured distribution. The origin of the resolution distortion is due to many instrument-specific factors which lead to an accumulation of (hopefully small!) uncertainties. These uncertainties have the general effect of *blurring* the overall response. The effects of instrumental resolution often can be quantified in the instrumental resolution function $R(Q, E)$. Mathematically, the resolution function and the intrinsic scattering function are convoluted to yield the measured response. We present here an example of a convolution of two functions and the effects of the resolution width.

In this example, we assume that the resolution function, $R(E)$, is a normalized Gaussian centered at zero:

$$R(E) = \frac{1}{\sqrt{2\pi\sigma^2}} e^{-\frac{E^2}{2\sigma^2}}. \tag{23}$$

The intrinsic scattering function $S(E)$ is a triangle function centered at zero with base Δ one unit wide ($\Delta = 1$) and unit height.

$$S(E) = \frac{2}{\Delta}\left[\left(E + \frac{\Delta}{2}\right)\Theta\left(E + \frac{\Delta}{2}\right) - 2E\Theta(E) + \left(E - \frac{\Delta}{2}\right)\Theta\left(E - \frac{\Delta}{2}\right)\right], \tag{24}$$

where Θ is the unit step function.

The measured response $I(E)$ is given by the convolution integral:

$$I(E) = S(E) \otimes R(E) = \int_{-\infty}^{+\infty} dE' S(E') R(E - E'). \tag{25}$$

When the Gaussian width σ is small, the Gaussian approaches a Dirac δ-function, and the resolution of the convolution looks very similar to the original triangle function. Figure 7 shows this result for a full-width at half-maximum (FWHM is approximately 2.3458σ) of 0.01. When the width is larger, the resulting convolution product looks more distorted and blurred. Figure 8 shows such a case when the resolution width is 0.5.

Note that as $R(E)$ becomes more narrow, the convolution product looks more like $S(E)$. For infinitely sharp resolution, $R(E) = \delta(E)$, the convolution product is *exactly* $S(E)$. Knowledge of the instrumental resolution function is essential for detailed lineshape analysis. Often this can be measured using an elastic scatterer.

In many cases, the instrumental resolution can be measured directly and used in the model fitting procedure *via* the convolution product. If we measure the scattering function from a purely elastic scatterer then the measured quantity is directly proportional to the resolution function. In particular, the elastic scattering function can be represented by a Dirac δ-function with area A: $S_{EL}(E) = A\delta(E)$. When convoluted with the resolution function, we get the measured response:

$$I_{\text{measured}}(E) = A \times \delta(E) \otimes R(E) = A \times R(E). \tag{26}$$

Note that we must normalize the resolution function so that it has unit area. This is necessary so that we can extract the integrated intensity of the intrinsic lineshape $S(E)$ from the fit to the model. Since the integrated intensity of the convolution product of two functions is equal to the product of the areas of the two functions, then, if one of these areas in unity, then the other must be the total area of the measured intensity.

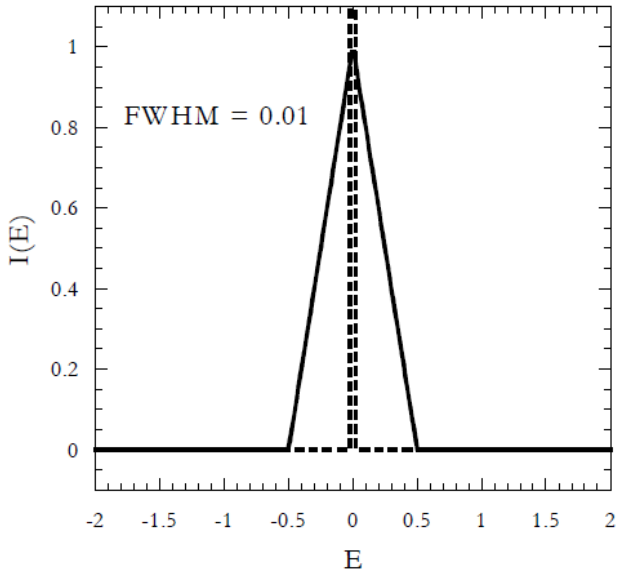

Figure 7: Result of the convolution of the triangle function with a Gaussian of width 0.01.

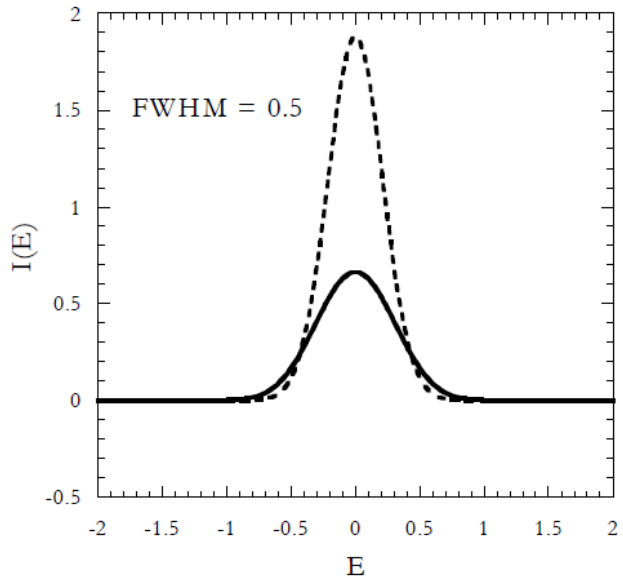

Figure 8: Result of convolution of the triangle function with a Gaussian of width 0.5.

References

[1] J. M. Carpenter and C.-K. Loong, *Elements of Slow Neutron Scattering: Basics, Techniques, and Applications* (Cambridge University Press, 2015).

[2] D. R. Cordray, L. R. Kaplan, P. M. Woyciesjes, and T. F. Kozak, "Solid-liquid phase diagram for ethylene glycol + water," *Fluid Ph. Equilibria* **117** 146-152 (1996).

[3] M. Matsugami, T. Takamuku, T. Otomo, and T. Yamaguichi, "Thermal Properties and Mixing State of Ethylene Glycol-Water Binary Solutions by Calorimetry, Large-Angle X-ray Scattering, and Small-Angle Neutron Scattering," *J. Phys. Chem. B*, **110**, 12372–12379 (2006).

[4] Yves Maréchal, *The Hydrogen Bond and the Water Molecule: The physics and chemistry of water, aqueous and bio media* (Elsevier, 2007).

[5] A. Meyer, R. M. Dimeo, P. M. Gehring, and D. A. Neumann, "The high-flux backscattering spectrometer at the NIST Center for Neutron Research," *Rev. Sci. Instrum.* **74**, 2759-2777 (2003).

[6] M. Bée, *Quasielastic Neutron Scattering: Principles and and Applications in Solid State Chemistry, Biology and Materials Science*, (IOP Publishing, 1988).

[7] A. Arbe, J. Colmenero, M. Monkenbusch, and D. Richter, "Dynamics of Glass-Forming Polymers: 'Homogeneous' versus 'Heterogeneous' Scenerios" *Phys. Rev. Lett.* **81**, 590-593 (1998).

[8] J. Wuttke, I. Chang, O. G. Randl, F. Fujara, and W. Petry, "Tagged-particle motion in viscous glycol: Diffusion-relaxation crossover," *Phys. Rev. E* **54**, 5364 (1996).